academicJournals

Vol. 8(18), pp. 698-704, 11 May, 2013
DOI: 10.5897/SRE12.577
ISSN 1992-2248 © 2013 Academic Journals
http://www.academicjournals.org/SRE

Scientific Research and Essays

Full Length Research Paper

Characterisation of two kaolin facies from Ediki, Southwest Cameroon

M. L. DIKO[1,*] and G. E. EKOSSE[2]

[1]Geology Division, University of Limpopo, Sovenga, P/B X1106 Limpopo Province, 0727 South Africa.
[2]Directorate of Research and Innovation, University of Venda, P/B X5050 Limpopo Province, 0950 South Africa.

Accepted 11 February, 2013

Sand-rich (ESR) and sand-poor kaolin (ESP) facies from Ediki, Southwest (SW) Cameroon, have been mineralogically and geochemically characterised in order to elucidate on their emplacement and degree of kaolinization. The mineralogical assemblage comprised quartz, kaolinite, muscovite, microcline, goethite and anatase. ESP registered a sharp peak at 3620 cm^{-1} and two weak inflections between the doublets at 3652 and 3670 cm^{-1}, whereas only one clearly resolved peak at 3620 cm^{-1} was observed for ESR. Quartz interference at 1023, 791 and 682 occurred in both samples. Laths, irregular platelets and flakes with swirl texture and corroded edges characterized ESR whereas loose stacks and flakes displaying a seemingly preferred orientation was observed in ESP. Low alumina content, CIA and high Si_2O_3:Al_2O_3 ratio coupled with relative enrichment of K over the other alkali and alkali earth metals was observed in both samples. The results infer partial kaolinization processes, low to moderate degrees of crystallinity and significant quartz contamination in both kaolin facies. The difference in mineralogy and geochemistry between the two facies is ascribed to physical controls on weathering (inferred porosity, permeability and inclination of the lithologic units) rather than the degree of chemical alteration.

Key words: Cameroon, kaolin facies, characterization, kaolinization.

INTRODUCTION

Kaolin [$Al_2Si_2O_5(OH)_4$] is a common phyllosilicate mineral, widely employed as raw material in ceramics, paper, filling, coating, refractory, fiberglass, cement, rubber and plastics, paint, catalyst, pharmaceutics and agriculture (Murray, 2007; Nkoumbou et al., 2009; Ekosse, 2010). The minerals of the kaolin group comprises kaolinite, dickite, nacrite, and halloysite of which kaolinite is the most common (Murray, 2007). Structurally they consist of the so-called 1:1 layers of combined silicate sheets (Si_2O_5) bonded to aluminium oxide/hydroxide [Al_2 $(OH)_4$] layers, which are continuous in the a- and b-axis directions and are stacked one above the other in the c-axis direction (Murray, 2007).

The use of kaolin in ceramic applications is accompanied by significant problems at different stages of its exploitation and product manufacturing; raw clay mining, processing, clay body formulation, drying, glazing, firing and cooling of finished product (Ekosse et al., 2007). Process-generated problems encountered during ceramic manufacture such as black coring, blistering, bloating, bubbles, crawling, crazing, exploding, fracturing, peeling, pin holing, shivering and warping can be traced back to the genetic history, mineral and chemical compositions as well as physico-chemical properties of the raw kaolin (Murray, 1999, 2000; Cravero et al., 2000; Ekosse, 2000, 2001, 2010; Saika et al., 2003; Gamiz et al., 2004; Dominguez et al., 2010; Diko et al., 2011; Diko and Ekosse, 2012). Efficient exploration

*Corresponding author. E-mail: dikom73@gmail.com. Tel: (+27) 071 347 6014. Fax: (+27) 015 268 3491.

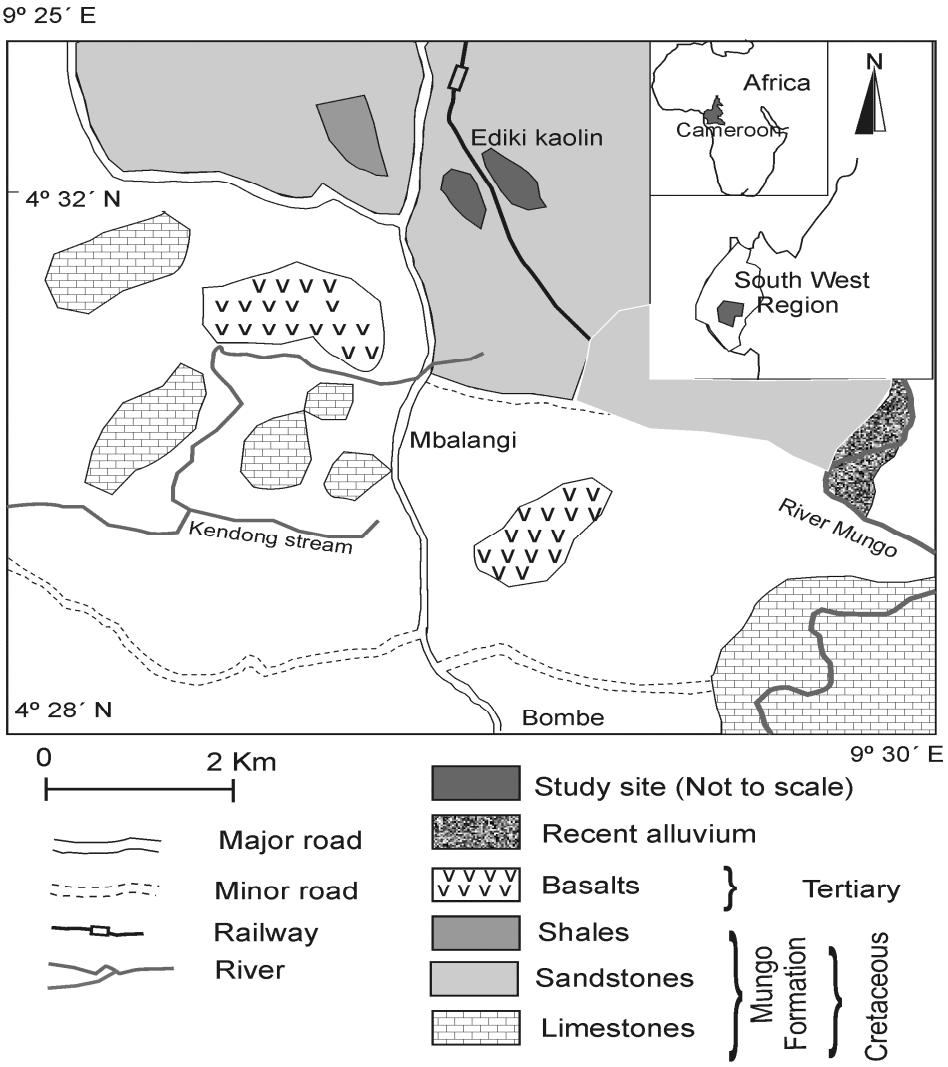

Figure 1. Location and geologic map of Ediki (Diko and Ekosse, 2012).

and exploitation of kaolin thus requires a proper understanding of its genesis and modes of formation (Murray, 2007).

In this study, two kaolin facies from Ediki kaolin occurrence, South West Region Cameroon have been mineralogically and geochemically characterised in order to elucidate on their emplacement mechanisms and degree of kaolinization.

Study area and geologic setting

The locality of Ediki in Meme Division, South West Cameroon is host to a kaolin occurrence situated along the Kumba-Mamfe highway (Figure 1) at longitudes 4° 28' 00" N – 4° 33' 00" N and latitude 9° 27' 00" E – 9° 30' 00" E (Diko and Ekosse, 2012). The kaolin crops out on two separate shale-bearing sandstone walls of about 15 to 20 m thick, separated by the Ediki Railway line.

Details of the geology of Ediki and lithostratigraphy of the kaolin occurrence have been discussed by Diko and Ekosse (2012). The kaolin occurs within the Mungo Formation of Upper Cretaceous age (Turonian – Cenomanian) and ascribed to the Douala Sedimentary Basin (Lakin, 2010). Within the vicinity of Ediki kaolin a dominantly sandstone unit covers the north and northeast. Further north of the study area, isolated shaley units are exposed whereas towards the centre and southeast, a significant limestone deposit occurs (Diko and Ekosse, 2012). Recent alluvium occurs towards the east particularly along the banks of River Mungo. Isolated basaltic rocks are exposed towards the north and centre of the study area. These Tertiary basalts appear to be undifferentiated (Diko and Ekosse, 2012).

The profile consists of upward coarsening kaolin bearing sandstone – siltstone – sandstone sequence (Figure 2), indicative of differential energy of depositional

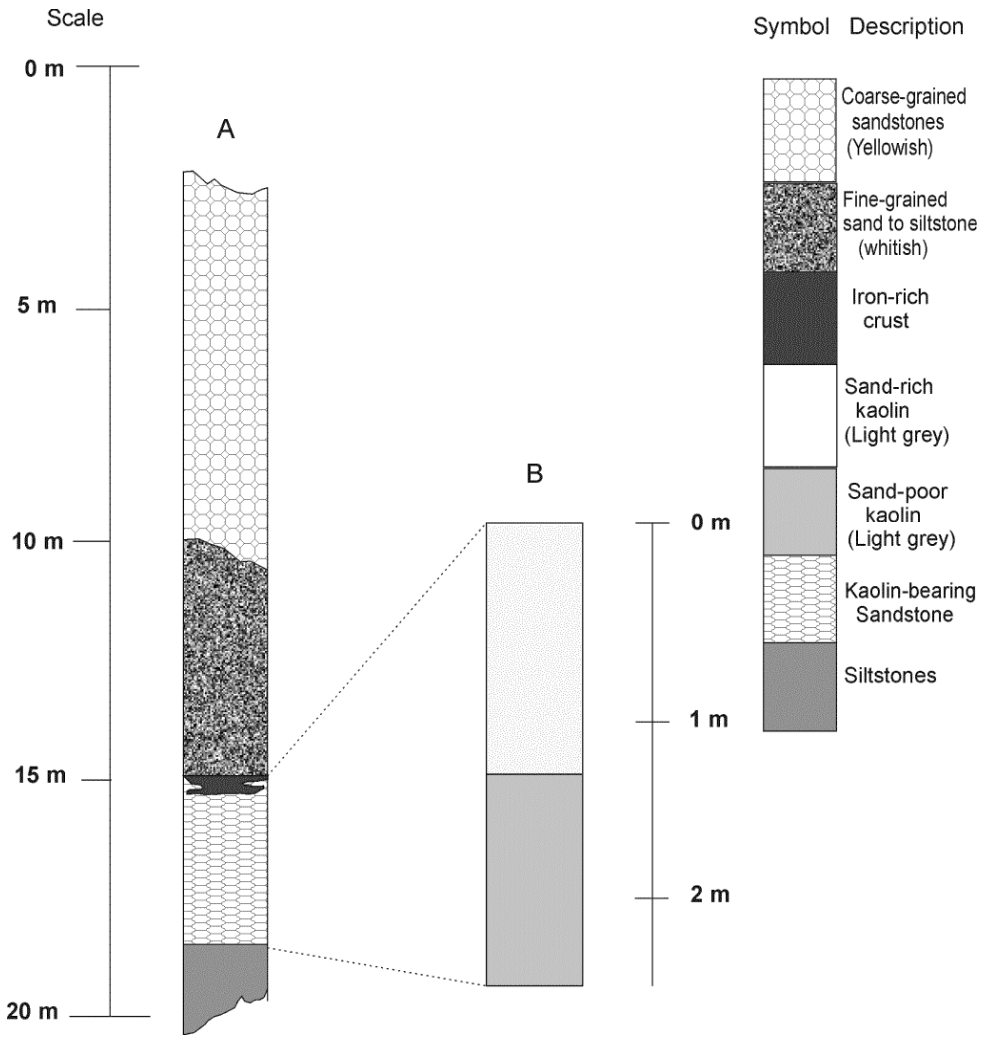

Figure 2. Lithostratigraphic profile (A) and representative kaolin profile (B) from Ediki kaolin (Diko and Ekosse, 2012).

environment and/or degree of weathering. The kaolin-bearing sandstone unit comprises a 2 to 3 m thick, highly weathered grey to greenish sandstone unit with dip of 35 to 40°. Overlying this unit is a thin lateritic crust (0.05 m) rich in iron oxides (goethite and/or hematite), followed by a fine-grained whitish sandstone horizon, approximately 4 m thick. Above this layer is a 7 m thick brown to yellowish, loosely packed coarse sand unit capped by a shallow top soil with variable thickness (0.4 m to ~ 1 m) across the length of the outcrop.

METHODOLOGY

A total of 8 representative samples (4 samples each from the two kaolin facies) were obtained for analysis. Powder X–ray diffraction (XRD) for bulk kaolin was carried out using a Philips PW 1710 XRD unit operated at 40 Kv and 30 mA, with a Cu-Kα radiation. A graphite monochromator with a PW 1877 Automated Power Diffraction, X'PERT Data Collector soft-ware package was employed for qualitative identification of the minerals.

The IR spectra for bulk kaolin were acquired using a Perkin Elmer system 2000 FTIR spectrophotometer at a resolution of 4 cm^{-1}. About 5 g of dried powdered samples were homogenized in spectrophotometric grade KBr in an agate mortar and pressed to 3 mm pellets with a hand press (Vaculíková et al., 2011). In order not to distort the crystallinity of kaolinite in the samples, the mixing was set to 3 min allowing for minimal grinding as suggested by Tan (1996). Peaks were reported based on percentage transmittance to given wavelengths.

Morphological analysis was performed using a JEOL JSM – 5800LV scanning electron microscope equipped with energy dispersive X-ray micro analysis (SEM-EDX). Samples were mounted on Al stumps using conductive glue. Excess particulate matter on the Al stumps was eliminated through vacuum spraying in order to minimize interference with the electrode during imaging. The Al stumps were coated with Au and viewed from the analytical scanning electron microscope (Ekosse, 2001). Particle images were obtained with the aid of a secondary electron detector.

Table 1. Qualitative mineralogy and major element geochemistry of bulk kaolin samples.

	Qualitative mineralogy					
	K	**Q**	**M**	**Mx**	**G**	**A**
ESR	++	+++	+	+++	+	+
ESP	+++	+++	++	++	+	+

	Major element geochemistry (wt %)											
	SiO_2	**Al_2O_3**	**Fe_2O_3**	**MnO**	**MgO**	**CaO**	**Na_2O**	**K_2O**	**TiO_2**	**LOI**	**Si/Al**	**CIA**
ESR	60.01	21.59	2.11	0.02	0.78	0.04	0.09	5.67	1.05	8.51	2.78	78.82
ESP	57.77	22.11	2.62	0.02	0.91	0.03	0.19	5.64	1.12	9.48	2.61	79.06
TK	46.3	39.8	–	–	–	–	–	–	–	13.9	1.81	–

(+++) Major, (++) minor, (+) trace, (–) Not detected: K-kaolinite; Q-quartz; M- muscovite; Mx-microcline; G-goethite; A-anatase; Fe_2O_3 (reported as total iron); CIA – chemical index of alteration; LOI – Loss on Ignition; TK-theoretical kaolinite (values obtained from Ekosse, 2001).

Bulk chemical analyses for major elements (SiO_2, Al_2O_3, Fe_2O_3, MnO, MgO, CaO, Na_2O, K_2O and TiO_2) as well as Loss on Ignition (LOI) were determined using a Philips PW 1404 X-ray dispersive fluorescence spectrometer (XRFS) following protocol described in Van Reeuwijk (2002). The Chemical index of alteration (CIA) (Nesbitt and Young, 1984) and SiO_2:Al_2O_3 ratios were computed as complementary parameters in ascertaining weathering intensity and degree of kaolinization (Murray 2007).

RESULTS AND DISCUSSION

As indicted earlier, a total of 8 samples were analysed, however due to the fact that there were very insignificant differences in mineralogical and geochemical data on all four samples from each facies type, only the results of one sample each depicting the two facies; sand-rich (denoted ESR) and sand-poor (denoted ESP) have been reported.

X-Ray diffractometry

A summary of the qualitative mineralogy is presented on Table 1. From the x-ray diffractogram (Figure 3) 111 kaolinite peak was absent in both samples whereas the 020 and 110 kaolinite peaks were observed. The characteristic mineralogical assemblage comprised quartz + kaolinite + muscovite + microcline + goethite + anatase. Kaolinite and microcline occurred as minor and major constituents in ESR respectively whereas kaolinite was a major phase in ESP. Quartz was a major phase in both samples with the most intense peaks observed at 24^o (4.24 Å) and 31^o (3.34 Å) (Figure 3). Two strong microcline peaks (3.23 and 3.24 Å) were observed at 17^o and 32^o for ESR whereas only one occurred for ESP. The absence of the 111 kaolinite peak in both representative samples suggests partial kaolinization, however relative enrichment of microcline in ESR compared to ESP infers more advanced argillic alteration in ESP as per equation (1).

$$2KAl_3SiO_3O_{10}(OH)_2 + 2H^+ + 3H_2O \rightarrow 3Al_2Si_2O_5(OH)_4 + 2K^+ \quad (1)$$

(microcline) (kaolinite)

IR Spectrometry

The structural order of kaolinites can be detected by differences in position and relative intensity of OH stretching and bending bands in IR spectrum (Vaculíková et al., 2011). The OH bands in kaolin typically display four sharp stretching bands between 3600 and 3700 cm^{-1} notably; 3697, 3670, 3652/50 and 3620 cm^{-1} (Ece et al., 2003; Saikia and Parthasarathy, 2010; Vaculíková et al., 2011). The strong band at 3697 cm^{-1} arises from surface hydroxyls and produces an in-phase vibration perpendicular to the 1:1 layers (Ece et al., 2003; Vaculíková et al., 2011). The two other bands at 3670 and 3652 cm^{-1} arise from stretching vibrations that are sub-parallel to the 1:1 layers whereas the low frequency 3620 cm^{-1} is assigned to the fourth OH inner group (Ece et al., 2003). According to Vaculíková et al. (2011) kaolinite structure is considered ordered; if the OH stretching and bending bands are clearly resolved; partially ordered; if the individual OH bands at 3670, 3650 and 938 cm^{-1} had low intensities but could be identified; and poorly ordered; if only one band near 3660 cm^{-1} or inflexions near 3670, 3650 and 938 cm^{-1} were observed in the spectra.

Infra-red spectra of representative bulk kaolin samples are shown on Figure 4. A sharp peak at 3620 cm^{-1} and two weak inflections between the doublets at 3652 and 3670 cm^{-1}, corresponding to OH stretching bands occurred in ESP, whereas only one clearly resolved peak at 3620 cm^{-1} was observed for ESR. H – O – H stretching bands at 3410 cm^{-1} and weak bending peaks at 1646 cm^{-1} ascribed to water of hydration was observed in both samples. Very weak Si – O stretching bands occurred at or close to 1113, 998, 789 and 682 cm^{-1} whereas Si – O deformation between 402 and 427 cm^{-1} (assigned to

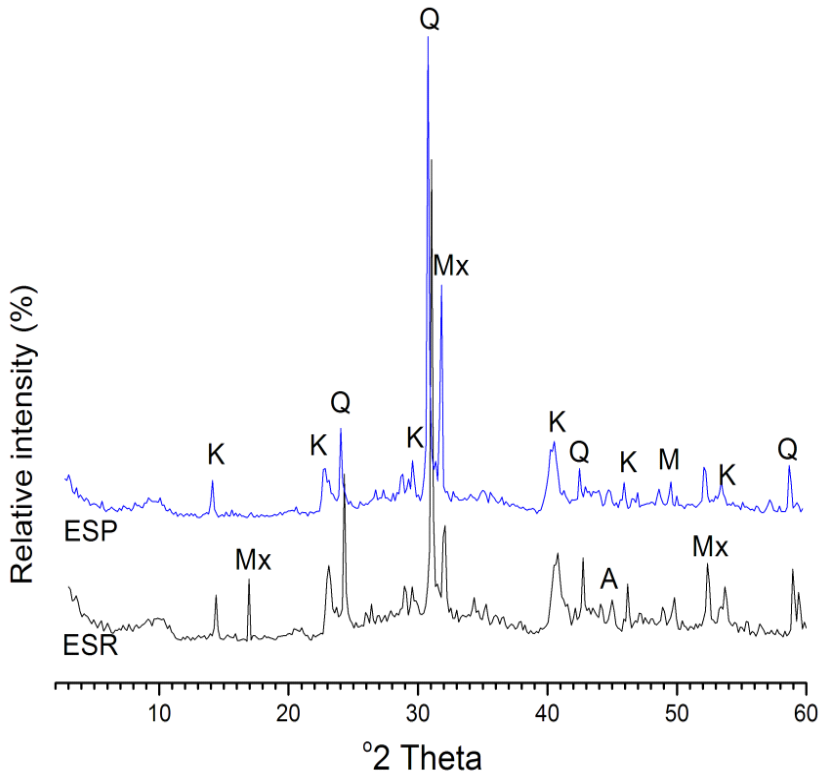

Figure 3. X-ray diffractogram of representative bulk kaolin samples (K: kaolinite, M: muscovite, Q: quartz, A: anatase, Mx: microcline).

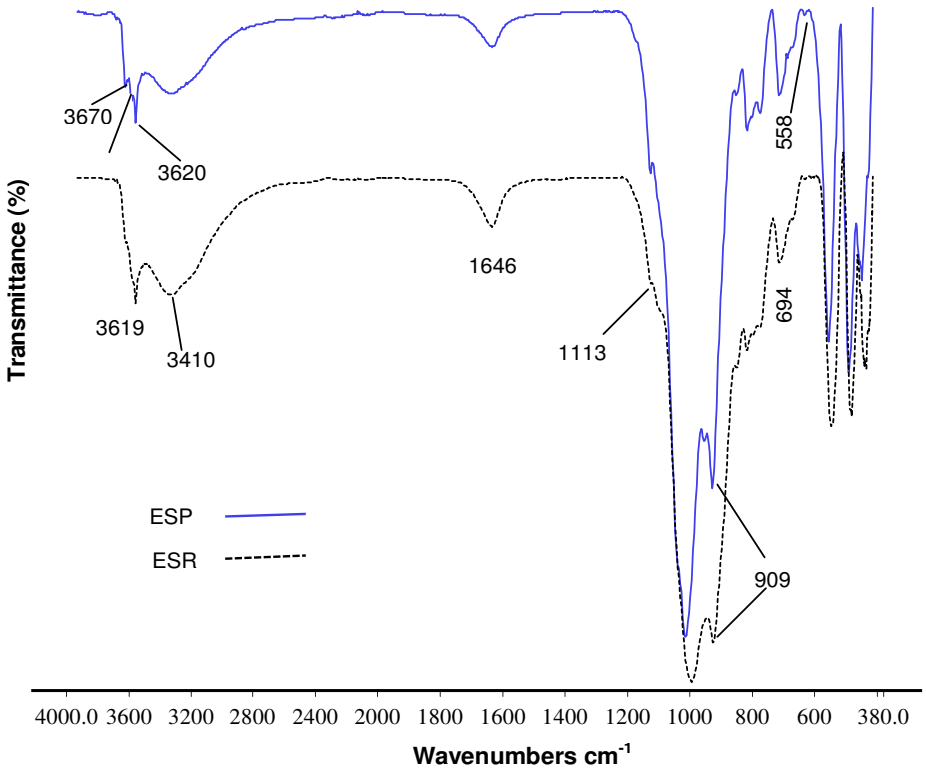

Figure 4. Infra-red spectra of representative bulk kaolin samples.

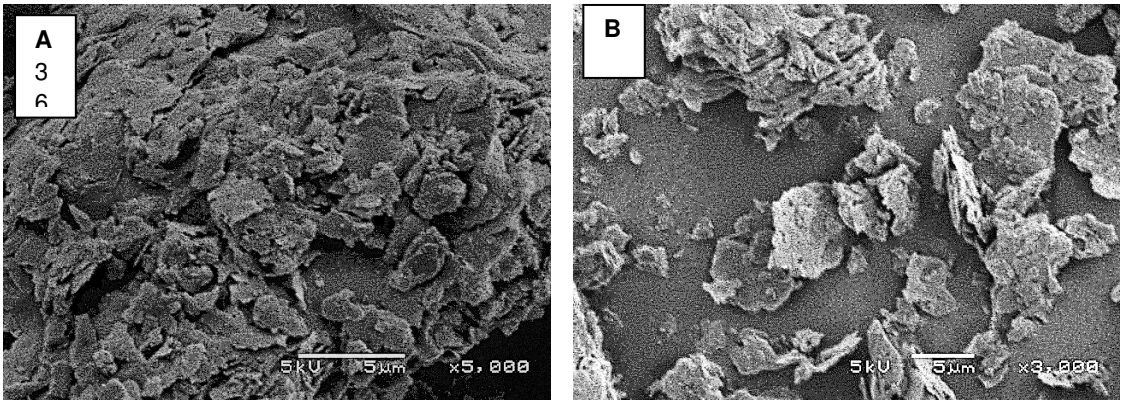

Figure 5. SEM photomicrograph of representative samples from Ediki kaolin occurrence; (a) laths, irregular platelets and flakes with swirl texture and rounded edges; (b) loose stacks and flakes.

microcline) occurred in both samples. Al---O-H deformation was ascribed within the region 907 to 910 cm¯1. Quartz interference at 1023, 791 and 682 (Vaculíková et al., 2011) was observed in both samples whereas a single very weak muscovite interference peak occurred only in ESP.

The transmittance bands and relative intensities are consistent with observed mineralogy. The single sharp OH stretching and associated weak doublets in ESP as opposed to the lone clearly resolved OH peak for ESR further confirms more advanced kaolinization and moderate structural order for the former (Ece et al., 2003; Saikia and Parthasarathy, 2010; Vaculíková 2011).

Kaolinite morphology

Morphologically, ESR was characterized by laths, irregular platelets and flakes with swirl texture and corroded edges (Figure 5a), whereas loose stacks and flakes displaying a seemingly preferred orientation was observed in ESP (Figure 5b). The occurrence of irregular platelets and flakes with signs of corroded edges further supports incomplete feldspar dissolution and kaolin precipitation. Based on the open texture of the kaolinite flakes and platelets associated with detrital feldspar grains, a secondary digenetic origin is proposed for Ediki kaolin (Lanson et al., 2002; Ruiz Cruz, 2007).

Major element geochemistry

Results of chemical analysis are summarized on Table 1. Alumina contents of the samples are lower than that for theoretical kaolinite whereas silica contents are higher. The samples equally show significant enrichment of K over the other alkali and alkali earth metals (Table 1) probably sourced from muscovite or feldspar mineral phases identified in the samples.

According to Roy et al. (2008) and, Mitchell and Sheldon (2009) CIA values for unaltered rocks and minerals are consistently around 50. Weathering products with CIA values < 60 suggests low chemical weathering, between 60 and 80, moderate whereas CIA values > 80 extreme chemical weathering (Roy et al., 2008). Based on the CIA values (Table 1), weathering intensity and degree of kaolinization is of moderate extent with a slightly more advanced alteration observed for ESP.

The Si_2O_3:Al_2O_3 ratio reflects the abundance of quartz and aluminosilicates in weathered products, with low Si_2O_3:Al_2O_3 values indicating relative enrichment of argillites at the expense of quartz and vice versa (Wu et al., 2011). The Si_2O_3:Al_2O_3 ratios of the studied kaolins are higher than the 1.18 value reported for theoretical kaolinite (Ekosse, 2001) (Table 1). The overall geochemistry of the two facies corroborates the mineralogical data and further supports partial kaolinization and immaturity of the argillaceous sediments.

Genesis and emplacement

Ediki kaolin is a dominantly sandstone hosted kaolin occurrence. The sandstones were derived from a k-feldspar rich source rock (probably dacite or rhyolite). Prior to kaolinization, quartz and feldspars sands that resulted from the weathering of felsic parent rocks were deposited in a locally developed basin (Mungo Formation), resulting in arkosic formations. Subsequent transformation of the k-feldspars to kaolinite in the two facies occurred in-situ. Despite the tropical climatic regime reported for Ediki (Ngole et al., 2007) the absence of the 111 kaolinite peak, relative enrichment of K over Ca, Na, Mg and Fe and low CIA observed in both representative samples, are consistent with incomplete or partial k-feldspar dissolution (Lanson et al., 2002). This observation further suggests that the effect of chemical weathering within the entire kaolin outcrop remained fairly constant throughout the period of deposition. However,

the differences in mineralogy and geochemistry observed between the two kaolin facies (Table 1) may be ascribed to physical controls (topography of the outcrop, degree of permeability and porosity) as opposed to degree of chemical alteration. A secondary digenetic emplacement mechanism is therefore suggested for the two kaolin facies on the basis of shallow depth at which kaolinization occurred; abundant detrital feldspars; some mica and quartz as well as inferred high porosity and permeability of the sandstones (Lanson et al., 2002; Bentabol et al., 2006; Ruiz Cruz, 2007).

Conclusion

Two kaolin facies from Ediki, SW Cameroon, have been chemically and mineralogically characterised to elucidate on their kaolinization process. The host sandstones contain, in addition to quartz, some detrital feldspars and mica grains which are favourable parent phases for kaolinite formation. However, the absence of the 111 kaolinite peaks and concomitant presence of well resolved quartz peaks, poorly resolved OH transmittance bands of very weak to moderate intensities, low alumina content, low CIA and high Si_2O_3:Al_2O_3 ratio coupled with relative enrichment of K over the other alkali and alkali earth metals, infers partial or incomplete kaolinization processes, low to moderate degrees of kaolinite crystallinity as well as significant quartz contamination in both kaolin facies. The occurrence of irregular platelets and flakes with signs of corroded edges further supports incomplete feldspar dissolution and kaolin precipitation. The difference in sand content between the two facies is ascribed to physical controls on weathering (inferred porosity, permeability and inclination of the lithologic units) rather than the degree of chemical alteration.

ACKNOWLEDGEMENTS

Funding from UNESCO/IUGS/ IGCP 545 Project on Clays and Clay Minerals in Africa is acknowledged.

REFERENCES

Cravero F, Keith KS, Murray HH, Toit T (2000). A white bentonite from San Juan Province, Argentina - Geology and potential industrial applications. Appl. Clay Sci. 16:31-34.

Diko ML, Ekosse GE (2012). Physico-chemical and mineralogical considerations of Ediki sandstone-hosted kaolin occurrence, South West Cameroon. Int. J. Phys. Sci. 7(3):501-507.

Diko ML, Ekosse GE, Ayonghe SN, Ntasin E (2011). Physical characterization of clayey materials from Tertiary volcanic cones in Limbe (Cameroon) for ceramic applications. Appl. Clay Sci. 51:380-384.

Dominguez EA, Iglesias C, Dondi M, Murray H (2010). Genesis of the La Espingarda kaolin deposit in Patagonia. Appl. Clay Sci. 47:290-302.

Ece OI, Nakagawa Z, Schroed P (2003). Alteration of Volcanic Rocks and Genesis of Kaolin Deposits in the Sile Region, Northern Istanbul, Turkey. I: Clay Mineralogy. Clays Clay Miner. 51(6):675-688.

Ekosse GE (2010). Kaolin deposits and occurrences in Africa: Geology, mineralogy and utilization. Appl. Clay Sci. 50 (2):212-236.

Ekosse GE (2000). The Makoro kaolin deposit, southeastern Botswana: Its genesis and possible industrial applications. Appl. Clay Sci. 16:301-320.

Ekosse GE (2001). Provenance of the Kgwakgwe kaolin deposit in southeastern Botswana and its possible utilization. Appl. Clay Sci. 20:137-152.

Ekosse GE, Mulaba A, Nkoma JS (2007). Physico-chemistry of continental bentonites and kaolin for ceramic applications. Afr. J. Sci. Technol. 8 (1):107-115.

Gamiz E, Melgoza M, Sanchez M, Martin-Garcia JM, Delgado R (2004). Relationship between chemico-mineralogical composition and colour properties in selected natural and calcined kaolin. Appl. Clay Sci. 28:269-282.

Lanson B, Beaufort D, Berger G, Bauer A, Cassagnabe` A, Meunier A (2002). Authigenic kaolin and illitic minerals during burial diagenesis of sandstones: A review. Clay Miner. 37:1-22.

Mitchell R, Sheldon, ND (2009). Weathering and paleosol formation in the 1.1Ga Keweenawan Rift. Precambrian Res. 168:271-283.

Murray HH (2007). Applied Clay Mineralogy. Occurrences, Processing and Application of Kaolins, Bentonites, Palygorskite-Sepiolite and Common Clays. Dev. Clay Sci. 2:179.

Murray HH (1999). Applied clay mineralogy today and tomorrow. Clay Miner. 34:39-49.

Murray HH (2000).Traditional and new applications for kaolin, smectite, palygorskite: A general overview. Appl. Clay Sci. 17:207-221.

Nesbitt HW, Young GM (1984). Prediction of some weathering trends of plutonic and volcanic rocks based on thermodynamic and kinetic considerations. Geochim. Cosmochim. Acta. 48:1523-1534.

Ngole VM, Ekosse GE, Ayonghe SM (2007). Physico-chemical, mineralogical and chemical considerations in understanding the 2001 Mabeta New Layout landslide, Cameroon. J. Appl. Sci. Environ. Manage. 11(2):201-208.

Nkoumbou C, Njoya A, Njoya D, Grosbois C, Njopwouo D, Yvon J, Martin F (2009). Kaolin from Mayouom (Western Cameroon): Industrial suitability evaluation. Appl. Clay Sci. 43:118-124.

Roy P, Caballero M, Lozano R, Smykatz-Kloss W (2008). Geochemistry of late quaternary sediments from Tecocomulco Lake, central Mexico: Implication to chemical weathering and provenance. Chemie der Erde. 68:383-393.

Ruiz Cruz MD (2007). Genesis and evolution of the kaolin-group minerals during the diagenesis and the beginning of metamorphism. In: Fernando Nieto and Juan Jiménez-Millán, (eds). "Diagenesis and Low-Temperature Metamorphism. Theory, Methods and Regional Aspects" Seminarios SEM. 3:41-52.

Saikia NJ, Bharali DJ, Sengupta P, Bordoloi D, Goswamee RL, Saikia PC, Borthakur PC (2003). Characterization, beneficiation and utilization of a kaolinite clay from Assam, India. Appl. Clay Sci. 24(1-2):93-103.

Saikia B, Parthasarathy G (2010). Fourier Transform Infrared Spectroscopic Characterization of Kaolinite from Assam and Meghalaya, Northeastern India. J. Mod. Phys. 1:206-210.

Tan KH (1996). Soil sampling preparation and analysis. Marcel Dekker Inc. New York, 392 pp.

Vaculíková L, Plevová E, Vallová S, Koutník I (2011). Characterization and differentiation of kaolinites from selected Czech deposits using infrared spectroscopy and differential thermal analysis. Acta Geod. Geomaterila. 8(161):59-67.

Van Reeuwijk LP (2002). Procedures for soil analysis. International Soil Reference and Information Centre, Wageningen, The Netherlands, Technical Paper 9, 101 pp.

Wu W, Xu S, Lu H, Yang J, Yin H, Liu W (2011). Mineralogy, major and trace element geochemistry of riverbed sediments in the headwaters of the Yangtze, Tongtian River and Jinsha River. J. Asian Earth Sci. 40:611-621.